

# Beyond 5G: Leveraging Cell Free TDD Massive MIMO using Cascaded Deep learning

Navaneet Athreya, Vishnu Raj and Sheetal Kalyani

**Abstract**—This paper deals with the calibration of Time Division Duplexing (TDD) reciprocity in an Orthogonal Frequency Division Multiplexing (OFDM) based Cell Free Massive MIMO system where the responses of the (Radio Frequency) RF chains render the end to end channel non-reciprocal, even though the physical wireless channel is reciprocal. We further address the non-availability of the uplink channel estimates at locations other than pilot subcarriers and propose a single-shot solution to estimate the downlink channel at all subcarriers from the uplink channel at selected pilot subcarriers. We propose a cascade of two Deep Neural Networks (DNN) to achieve the objective. The proposed method is easily scalable and removes the need for relative reciprocity calibration based on the cooperation of antennas, which usually introduces dependency in Cell Free Massive MIMO systems.

**Index Terms**—Cell Free Massive MIMO, Deep Learning, Channel Reciprocity

## I. INTRODUCTION

Cell Free MIMO is a potential paradigm shift in wireless network design for 5G and beyond that includes the benefits of Massive MIMO as well as ability to exploit diversity and increase the immunity against shadow fading [1]. However, the technology is still limited by many practical constraints such as channel non-reciprocity [1].

Even though most MIMO systems operate in TDD mode, the end to end channel is typically rendered *non-reciprocal* because of the RF front ends and usually careful calibration is required to achieve reciprocity [2]. The impact of non-reciprocal channels on the gains of Cell Free Massive MIMO is analysed in [3]. Even in the presence of reciprocity, the acquisition of the complete Downlink CSI from the Uplink CSI is not very straightforward, due to the non availability of Uplink CSI in the subcarriers which don't have reference signals.

Popular approaches for TDD reciprocity calibration are based on internal BS sounding using dedicated RF circuitry or over the air sounding among the Access Points (APs) which requires coordination [2], [4], [5]. Most of these methods are only relative calibration methods that achieve reciprocity up to a multiplicative constant, which needs to be estimated [4]. The main limitation on application of traditional calibration methods to a Cell Free Massive MIMO setting is the need for over the air sounding and requirement of stringent synchronization between the APs, which often is very hard since there is no centralized reference clocks for these APs. Hence, it is desirable to have an approach in which each AP has full

control over its local CSI, rather than relying on the other APs to acquire its CSI.

Most works in Cell Free Massive MIMO also focus on narrowband communication and assume that pilots are only multiplexed in the code domain as orthogonal reference signals. But, many cellular standards such as 5G, adopt Multicarrier schemes and use pilot aided methods for channel estimation, where the pilots are multiplexed in both the code domain as well as the frequency domain [6]. In a comb type pilot structure, reference signals (pilots) are inserted at specific subcarriers in the grid, and the pilot signals are frequency multiplexed among users [6]. It is possible to estimate the CSI at the pilot subcarriers using standard estimation methods. However, at the subcarriers that do not have reference signals, which we call as *blind subcarriers*, it is difficult to estimate highly accurate CSI without any prior knowledge, such as the second order statistics for an MMSE estimator [7]. Hence, limited resource elements in reference signals for channel estimation makes it hard to obtain accurate CSI required for achieving high data rates.

A popular approach to combat the non-availability of CSI at blind subcarriers is frequency domain interpolation. But linear interpolation methods typically require dense pilots, which in turn reduces the spectral efficiency. Thus it might be desirable to have powerful non-linear interpolators. The combination of Reciprocity calibration as well as Frequency Domain interpolation is clearly a nonlinear problem, when assuming that pilots are sparse.

Artificial Neural Networks (ANNs) are widely used as non-linear function approximators and application of deep learning methods to problems in wireless communication systems has become popular recently due to its competitive performance. Deep learning has been successfully applied in the problems of communication systems design [8]–[10], OFDM systems [11] etc. In this work, we present a cascaded deep learning based method for inter-pilot interpolation and TDD reciprocity calibration in Cell Free Massive MIMO systems.

Major contributions of this work are

- 1) A novel combined method for TDD-reciprocity calibration and CSI interpolation using deep learning to recover the Downlink CSI across the entire Bandwidth part from the Uplink CSI obtained at a small number of pilot subcarriers.
- 2) A scalable and intelligent system for Cell Free Massive MIMO that identifies the frequency selectivity of the environment of operation and performs accurate interpolation accordingly.

Navaneet Athreya is with Department of ECE, Virginia Tech, Blacksburg, VA, USA (e-mail: navaneet@vt.edu).

Vishnu Raj and Sheetal Kalyani are with the Department of Electrical Engineering at IIT Madras, Chennai, India (e-mail: {ee14d213, skalyani}@ee.iitm.ac.in).

### A. Notations

Bold face upper case (eg.  $\mathbf{A}$ ) bold lower case letters denotes  $\mathbf{b}$  matrix and column vectors respectively. Inverse of a matrix  $\mathbf{A}$  is denoted by  $\mathbf{A}^{-1}$  and transpose by  $\mathbf{A}^T$ . Element at  $i^{th}$  row  $j^{th}$  column of matrix  $\mathbf{A}$  is denoted by  $a^{(ij)}$ .

## II. SYSTEM MODEL

Consider a multicarrier system of  $N$  subcarriers with  $M$  APs and  $K$  UEs. There are a total of  $M \times K$  channels for each of the  $n$  ( $n = 1, 2, \dots, N$ ) subcarriers. We assume perfect synchronization and coordinated communication.

Let  $\mathbf{x}_{UL} \in \mathbb{C}^{K \times 1}$  and  $\mathbf{x}_{DL} \in \mathbb{C}^{M \times 1}$  be the transmit symbols on the one subcarrier during uplink and downlink respectively. The received symbols for uplink and downlink can then be written as

$$\mathbf{y}_{UL} = \mathbf{H}_{UL}\mathbf{x}_{UL} + \mathbf{w}_{UL} \quad (1)$$

$$\mathbf{y}_{DL} = \mathbf{H}_{DL}\mathbf{x}_{DL} + \mathbf{w}_{DL}, \quad (2)$$

where  $\mathbf{H}_{UL} \in \mathbb{C}^{M \times K}$  and  $\mathbf{H}_{DL} \in \mathbb{C}^{K \times M}$  are the uplink and downlink channels respectively for that subcarrier and  $\mathbf{w}$  is the corresponding AWGN noise. The channels  $\mathbf{H}_{UL}$  and  $\mathbf{H}_{DL}$  will include the effects from the RF front-end at both the transmitter and receiver. These effects can be captured using the model [2]

$$\mathbf{H}_{UL} = \mathbf{R}_{UL}\mathbf{C}_{UL}\mathbf{T}_{UL} \quad (3)$$

$$\mathbf{H}_{DL} = \mathbf{R}_{DL}\mathbf{C}_{DL}\mathbf{T}_{DL} \quad (4)$$

where  $\mathbf{T}_{UL} \in \mathbb{C}^{K \times K}$ ,  $\mathbf{R}_{DL} \in \mathbb{C}^{K \times K}$ ,  $\mathbf{T}_{DL} \in \mathbb{C}^{M \times M}$  and  $\mathbf{R}_{UL} \in \mathbb{C}^{M \times M}$  and are the RF transmitter and receiver chains of the UE and BS respectively. The diagonal elements in  $\mathbf{T}_{DL}, \mathbf{R}_{DL}, \mathbf{T}_{UL}, \mathbf{R}_{UL}$  correspond to the gains of individual chains and the off-diagonal elements corresponds to RF-cross talk and antenna coupling. Here,  $\mathbf{C}_{UL}$  and  $\mathbf{C}_{DL}$  are the physical wireless channels between the RF front-ends of BS and UE. The  $(m, k)^{th}$  element of  $\mathbf{C}_{UL}$ ,  $g_{m,k}$  is modelled as [1],  $g_{m,k} = \sqrt{\beta_{m,k}}h_{m,k}$ , where  $\beta_{m,k}$  represents the large scale fading and  $h_{m,k} \sim \mathcal{CN}(0, 1)$  represents the small scale fading.

We assume that the RF chains are Linear Time Invariant (LTI). Assuming TDD mode of operation, the wireless channel is reciprocal for every link between BS and UE. Hence, we have  $\mathbf{C}_{DL} = (\mathbf{C}_{UL})^T$ . Under the assumption the RF front end matrices are invertible, the downlink channel  $\mathbf{H}_{DL}$  can be decomposed as

$$\begin{aligned} \mathbf{H}_{DL} &= \mathbf{R}_{DL}\mathbf{C}_{DL}\mathbf{T}_{DL} \\ &= \mathbf{R}_{DL}(\mathbf{R}_{UL}^{-1}\mathbf{H}_{UL}\mathbf{T}_{UL}^{-1})^T\mathbf{T}_{DL} \\ &= \mathbf{R}_{DL}(\mathbf{T}_{UL}^{-1})^T(\mathbf{H}_{UL})^T(\mathbf{R}_{UL}^{-1})^T\mathbf{T}_{DL} \end{aligned} \quad (5)$$

Hence, with channel reciprocity, the downlink channel  $\mathbf{H}_{DL}$  can be computed as a transformation of the uplink channel  $\mathbf{H}_{UL}$ . However, for the estimation of  $\mathbf{H}_{DL}$ , perfect knowledge of RF front end matrices are required. In practical cases, this information is not easily available and traditional methods resort to internal sounding based techniques [2], [4], [5].

### A. OFDM based Cell Free Massive MIMO

Orthogonal Frequency Division Multiplexing (OFDM) is a popular multicarrier scheme that is used in current wireless standards such as 5G-NR and 4G-LTE. We consider a Cell Free Massive MIMO based system with OFDM scheme. At an individual single antenna transmitter, an OFDM frame is built by inserting pilots in to the data-block and then taking inverse discrete Fourier transform (IDFT) to convert the signal from frequency domain to time domain. Then a cyclic prefix (CP), of length no shorter than delay spread, is inserted before transmission. At a single AP  $m$ , the transmitted frequency domain signal in the Downlink to a single UE  $k$  can be represented as

$$y_{DL}(n) = g_{mk,DL}(n)x_{DL}(n) + w_{DL}(n), \quad n = 1, \dots, N, \quad (6)$$

where  $N$  is the block length (number of sub-carriers) of OFDM block. The precoding for a Downlink OFDM block requires  $g_{mk,DL}$  at each sub-carrier, which needs to be obtained from the Uplink CSI. The absence of perfect CSI due to channel estimation error or non-reciprocity degrades the performance of Massive MIMO and could inhibit one from realizing it's full potential [12]. Assuming we know the Uplink CSI at the pilot subcarriers, the Downlink CSI at all the blind subcarriers need to be estimated.

For a single link between the  $m^{th}$  AP and the  $k^{th}$  UE, the Downlink channel  $g_{mk,DL}$  at the  $n^{th}$  subcarrier could be written as:

$$g_{mk,DL}(n) = f\left(\frac{r_{DL}(l)t_{DL}(l)}{r_{UL}(l)t_{UL}(l)}g_{mk,UL}(l)\right) \quad (7)$$

Here the function  $f(\cdot)$  between channel at a blind subcarrier  $n$  and a pilot subcarrier  $l$  is induced mainly by the wireless channel, which is nothing but a measure of frequency selectivity of the channel.

## III. PROPOSED APPROACH

From (7), we can see that for a single channel between a UE and an AP, process of predicting the Downlink CSI at all subcarriers from the Uplink channel estimates at pilot positions involves both reciprocity calibration and frequency domain interpolation. Using Deep learning, one could approximate the downlink channel at all subcarriers from the uplink channel at pilot subcarriers. Even though the RF chain responses could be assumed to be roughly constant for a long time [3], the function induced by the wireless channel depends on the scenario. Modern wireless standards require the devices to operate in multiple scenarios of operation such as Indoor Hotspot, Urban, Rural, etc and the frequency selectivity differs across scenarios. Since it is essential that an interpolation function works for every scenario, one needs to learn the type of frequency selectivity in the current scenario. We assume that there are  $S$  classes of channels, with each class having different Power Delay Profile (PDP).

Hence, (7) now becomes:

$$g_{mk,DL}(n) = f_s\left(\frac{r_{DL}(l)t_{DL}(l)}{r_{UL}(l)t_{UL}(l)}g_{mk,UL}(l)\right)\mathbf{i}(g_{mk,UL} \in s) \quad (8)$$

where  $i(g_{mk,UL}) \in \{0, 1\}$  is an indicator variable to indicate which of the  $S$  classes the channel belongs to. The indicator variable for the  $s$ th class is 1 and the variables for the other  $S - 1$  classes are 0 if the channel  $i(g_{mk,UL})$  belongs to the  $s$ th class.

### A. Channel Identification

Since the frequency domain correlation of the channel is the fourier transform of the PDP, it can be understood that PDP determines the function  $f_s(\cdot)$  in (8). Since the PDP changes across scenarios, the first step in the proposed method is to classify the Uplink channel estimates into one of the known channel classes/scenarios based on the PDP using the CSI from pilot positions. The classifier performs the role of the indicator.

We assume that each block of the Uplink transmitted data is inserted with  $N$  pilots. Upon reception of the block, we can obtain the CSI at each of these pilot positions through any of the standard channel estimation methods [7]. This information is then fed to a neural network based classifier for channel identification. Since neural networks can only work with real numbers, we flatten the complex CSI information into real and imaginary parts and feed it to the classifier network. Thus the neural network takes in an input vector of dimension  $2N$ . The output layer of the network is of dimension  $S$  with softmax activation function, computing a surrogate probability of the provided sample being in each of the class. During training phase, samples from different channel scenarios are used with corresponding one-hot labeling for class. Categorical cross entropy is used as the loss function to train the classifier.

### B. Interpolation and Reciprocity Calibration

We combine the process of interpolation and TDD reciprocity calibration into one step and train a deep neural network (DNN) with this objective. We train  $S$  different DNNs for this purpose; one for each of  $S$  class of channels identified during the system modelling. Each DNN is trained to take a  $2N$  dimensional input, corresponding to the flattened CSI information from the pilot positions. The output is of dimension  $2K$  corresponding to the real and imaginary parts of the downlink channel which includes both the calibration and interpolation. During training, the CSI information along with the actual downlink channel information from the corresponding channel class is fed to the network. We used mean squared error as the loss function to train the network.

A schematic representation of the proposed *TDDNet* approach is given in Fig. 1. In a practical situation, the CSI information that can be estimated includes the wireless channel impairments and RF impairments at both transmitter and receiver. Hence, we propose to use the data which includes these impairments as this the closest we can get to practical scenarios. More specifically, we use the UL CSI which includes the RF impairments at both the AP and UE to predict the DL CSI which also includes the RF impairments at both the sides as the input. During the training phase, the classifier network and the calibration DNNs are individually trained. During testing, the samples are first fed to classifier network, which activates one of the calibration networks based on the

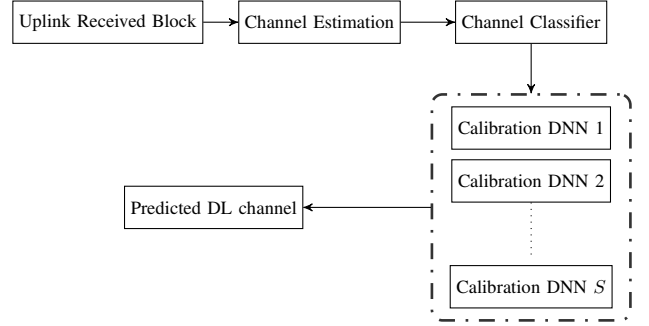


Fig. 1: Schematic of the proposed TDDNet scheme.

---

### Algorithm 1 Algorithm for Downlink Channel prediction

---

- 1: **Input:** Received uplink pilot block  $y_{P,UL}$
  - 2: **Output:** Downlink CSI  $h_{DL}$
  - 3: **for** Each received block **do**
  - 4:   Compute Uplink channel at pilot positions as  $h_{P,UL}(n) = y_{UL}(n)/x_{UL}(n)$  where  $x_{UL}(n)$  is the known pilot symbol at the  $n$ th subcarrier and  $h_{P,UL}$  is a vector of uplink channel estimates at pilot positions.
  - 5:   Classify  $h_{P,UL}$  to one of the known channel classes using the classifier network.
  - 6:   Select appropriate downlink channel prediction DNN based on the output of the classifier.
  - 7:   Use  $h_{P,UL}$  and the selected DNN to predict the downlink channel  $h_{DL}$  for all subcarriers.
  - 8: **end for**
- 

detected channel profile and the downlink CSI is predicted for all subcarriers by the model. An algorithmic description of the proposed method is provided in Alg. 1.

### C. Scaling up for Multiple links

In a Cell Free scenario, there are multiple links which can be assumed to be i.i.d due to the distribution of APs and UEs. In this case, our method is easily scalable since each AP does not have to depend on the other APs for calibration, in contrary to the traditional relative calibration schemes in which each AP has to coordinate with other APs to achieve reciprocity. Usually traditional calibration is achieved by having a reference RF chain among the operating RF chains and sounding calibration signals to the reference chain [13] [4]. By obviating the dependence of APs, over the air transmission of reference signals among APs is not required. This means that as and when new APs are added to the network, there is no disruption caused to it by the operating APs. Such an independence is crucial to the flexibility offered by Cell Free systems.

The proposed method of calibration on a per link basis also applies to multiple UEs since each UE might have a unique RF chain response and each AP is required to calibrate reciprocity individually with each of the UEs.

## IV. EXPERIMENTAL RESULTS

This section presents the results comparing the proposed method with popular approaches present in literature. For

evaluation, we have identified 5 channel classes based on (3GPP) TR 38.901 Release 15 [14] Channel models viz.: TDL-A, TDL-B, TDL-C, TDL-D, TDL-E. We followed Sec 7.7.5.2 of TR 38.901 Release 15 to use the TDL models for MIMO channels. Each of these classes has different delay profile and thus a different frequency structure. We consider 256 subcarriers with 30KHz subcarrier spacing. The carrier frequency is set to 3.5GHz and the sampling frequency is 100MHz. For modelling a moderate time selectivity, we used a UE velocity of 20kmph for all simulations. The gains of RF chains across subcarriers has been modelled as i.i.d random variables distributed as  $X \sim \mathcal{CN}(g_m, \sigma^2)$  (where  $g_m$  is the average baseband gain of the RF chain and  $\sigma^2$  is the variance), and are kept constant throughout the experiment. The wireless channels and RF chains were generated using MATLAB and the 5G toolbox of MATLAB.

During the training phase, samples of the Uplink CSI from pilot positions from different channel models are labeled and used to train the classifier network. For comparing the MSE performance of the proposed approach across SNR, we used a system with 256 subcarriers out of which 11 are pilots. We split the complex Uplink CSI information into two real numbers and stack them together to form a 22 dimensional input vector for the system. Similarly, the output from the network is a 512 dimensional real vector which we reshape into a 256 dimensional complex vector for obtaining the downlink CSI. The details for training classifier network is given in Table I. The Downlink channel prediction network is trained specifically, one for each channel class. Details for training the network are given in Table II.

Parameter	Value
Input dimension	22
Hidden Layer 1	22 (tanh)
Hidden Layer 2	22 (sigmoid)
Output dimension	5 (softmax)
Loss	Cross Entropy

TABLE I: Parameters for classifier network

Parameter	Value
Input Dimension	22
Hidden Layer 1	512 (tanh)
Hidden Layer 2	128 (tanh)
Output Layer	512 (linear)
Loss	MSE

TABLE II: Parameters for channel prediction network

The first step in the proposed approach is the classification of observed channel samples into one of the pre-identified classes. Fig. 2 highlights the necessity of an accurate classifier at the first stage, and justifies the cascade approach. In this experiment, a DNN trained for TDL-A channel model is used for predicting the downlink channel for different channel models. Without a classifier, the mismatch in the PDP increases the MSE as shown in the figure. Similar observations can also be made for other channel models also.

As the first part of the cascaded architecture, the classifier network needs to have high accuracy to correctly classify the channel samples across a wide range of SNR. Fig. 3

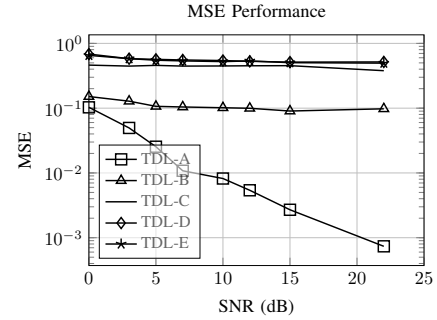


Fig. 2: MSE when all channels are predicted using TDL-A model.

provides the classification accuracy of the trained network across different SNR. At low SNR, the signal strength received may not be enough to correctly identify the Power Delay Profile (PDP) of the channel and hence we see a drop in accuracy at lower SNRs. However, even in low SNR, the trained network is able to correctly classify the PDPs of the channel with more that 60% accuracy.

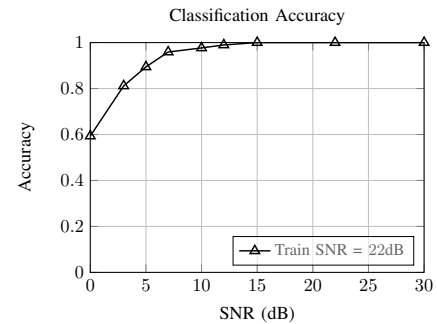


Fig. 3: Accuracy plot classifier network at different SNR (dB).

A comparison of results of the proposed system is given in Fig. 4. The MSE of the proposed cascaded approach for different channel models are given in Fig. 4a. A pilot spacing of 24 subcarriers is used. We can observe the proposed method shows similar trend in performance for all channel models. The dotted line is the MSE performance of an oracle classifier which always classifies the channel samples correctly and activates the *correct* interpolation/calibration DNN for Downlink channel prediction. We can observe that the MSE performance of oracle is slightly better than the proposed method at lower SNRs. The accuracy of classifier is not 100% at lower SNRs and this why the proposed cascade method incurs slightly higher MSE at that regime.

The effect of Uplink pilot spacing for Downlink channel prediction is studied in Fig. 4b for the TDL-C channel type at 22 dB SNR. The proposed method is compared against popular Linear interpolation method and Wiener Filter (Linear MMSE assuming perfect knowledge about second order statistics of the channel) based interpolation method. We can observe that both Linear and Wiener Filter based interpolation are sensitive to Uplink pilot spacing while the proposed method is robust to this.

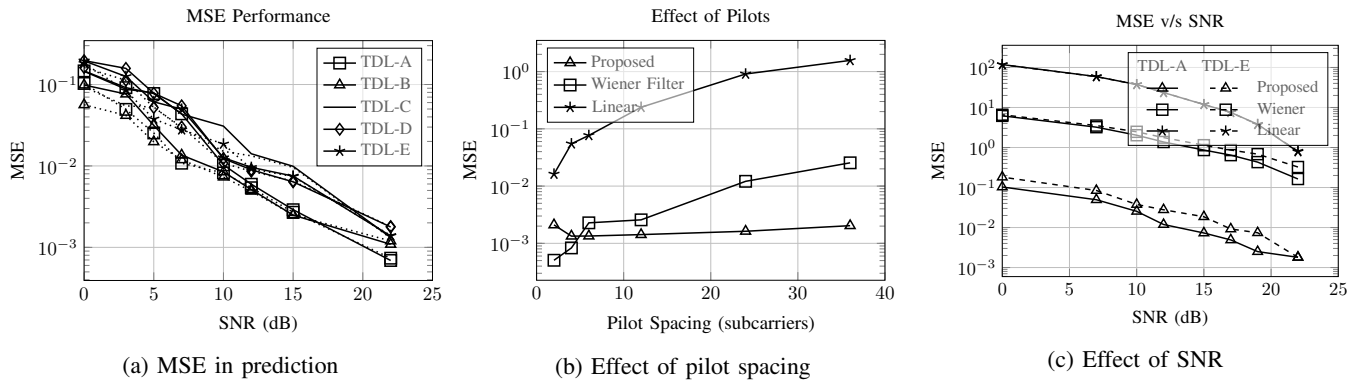


Fig. 4: Performance of proposed approach

The MSE performance of the methods under comparison with sparse pilot scenario is given in Fig. 4c. We used a pilot spacing of 24 in 256 subcarrier system. This results in a total of 11 pilots. It can be clearly observed that the proposed method provides better estimation of downlink channel even with sparse pilots, while the traditional methods (Linear and Wiener filter methods) suffer with high MSE. This improvement in MSE even in sparse pilot scenario can be attributed to the capabilities of neural networks to perform high resolution approximation of non-linear functions.

## V. CONCLUDING REMARKS

We discussed the problem of Downlink CSI acquisition from the Uplink CSI in a Cell Free Massive MIMO scenario and proposed a method using Deep learning to solve it. We presented a method for reciprocity calibration and obtaining the complete channel estimate for precoding purposes using a cascade of DNNs. Results indicate that our method outperforms traditional methods significantly even with a few number of pilots, thus providing better spectral efficiency. Even though we discussed the utility of cascaded deep learning based channel estimation in the context of TDD Cell Free Massive MIMO, the proposed method can be applied to systems which otherwise require the User Equipment(UE) to estimate downlink CSI.

## VI. ACKNOWLEDGEMENT

The authors would like to thank Dr. Radhakrishna Ganti, Associate Professor of Electrical Engineering, IIT Madras for useful discussion.

## REFERENCES

- [1] H. Q. Ngo, A. Ashikhmin, E. G. Larsson, and T. L. Marzetta, "Cell Free Massive MIMO versus Small Cells," *IEEE Communications Magazine*, vol. 52, no. 2, pp. 186–195, 2014.
- [2] J. Vieira, F. Rusek, O. Edfors, S. Malkowsky, L. Liu, and F. Tufvesson, "Reciprocity calibration for massive MIMO: Proposal, modeling, and validation," *IEEE Transactions on Wireless Communications*, vol. 16, no. 5, pp. 3042–3056, 2017.
- [3] J. M. Palacios, O. Raeesi, A. Gokceoglu, and M. Valkama, "Impact of Channel Non-Reciprocity in Cell-Free Massive MIMO," *IEEE Wireless Communications Letters*, pp. 1–1, 2019.
- [4] C. Shepard, H. Yu, N. Anand, E. Li, T. Marzetta, R. Yang, and L. Zhong, "Argos: Practical many-antenna base stations," in *Proceedings of the 18th annual international conference on Mobile computing and networking*. ACM, 2012, pp. 53–64.
- [5] X. Jiang, A. Decurvinge, K. Gopala, F. Kaltenberger, M. Guillaud, D. Stock, and L. Deneire, "A framework for over-the-air reciprocity calibration for TDD massive MIMO systems," *IEEE Transactions on Wireless Communications*, vol. 17, no. 9, pp. 5975–5990, 2018.
- [6] E. Dahlman, S. Parkvall, and J. Skold, *5G NR: The next generation wireless access technology*. Academic Press, 2018.
- [7] S. Coleri, M. Ergen, A. Puri, and A. Bahai, "Channel estimation techniques based on pilot arrangement in OFDM systems," *IEEE Transactions on broadcasting*, vol. 48, no. 3, pp. 223–229, 2002.
- [8] T. O'Shea and J. Hoydis, "An introduction to deep learning for the physical layer," *IEEE Transactions on Cognitive Communications and Networking*, vol. 3, no. 4, pp. 563–575, 2017.
- [9] H. Ye, G. Y. Li, and B.-H. Juang, "Power of deep learning for channel estimation and signal detection in OFDM systems," *IEEE Wireless Communications Letters*, vol. 7, no. 1, pp. 114–117, 2018.
- [10] V. Raj and S. Kalyani, "Backpropagating through the air: Deep learning at physical layer without channel models," *IEEE Communications Letters*, vol. 22, no. 11, pp. 2278–2281, 2018.
- [11] X. Gao, S. Jin, C.-K. Wen, and G. Y. Li, "ComNet: Combination of deep learning and expert knowledge in OFDM receivers," *IEEE Communications Letters*, vol. 22, no. 12, pp. 2627–2630, 2018.
- [12] D. Mi, M. Dianati, L. Zhang, S. Muhaidat, and R. Tafazolli, "Massive MIMO performance with imperfect channel reciprocity and channel estimation error," *IEEE Transactions on Communications*, vol. 65, no. 9, pp. 3734–3749, 2017.
- [13] T. L. Marzetta, "Noncooperative cellular wireless with unlimited numbers of base station antennas," *IEEE Transactions on Wireless Communications*, vol. 9, no. 11, p. 3590, 2010.
- [14] 3GPP, "Study on channel model for frequencies from 0.5 to 100 GHz 3rd generation partnership project (3gpp), tr 38.901 v15.0.0," 2018.